Stochastic and Deterministic Resonances for Excitable Systems

André Longtin[1] and Dante R. Chialvo[2]
[1]*Département de Physique, Université d'Ottawa, 150 Louis Pasteur, Ottawa, Ontario, Canada K1N 6N5*
[2]*Center for Studies in Physics and Biology, Rockefeller University, 1230 York Avenue, New York, New York 10021*
(Received 31 December 1997)

The dependence of four firing statistics in neuronal excitable systems is studied as a function of noise intensity and sinusoidal forcing period. For a range of biologically relevant frequencies, we find that the noise amplitude optimizing these statistics depends on the forcing period T, and that stochastic resonance with time-scale matching occurs. Results are explained by the interplay of generic static and dynamic threshold properties of excitable systems. [S0031-9007(98)07562-0]

PACS numbers: 87.22.Jb, 05.40.+j

Excitable dynamics underlie the behavior of many systems ranging from Josephson junctions, to chemical reactions to cardiac and nerve cells [1,2]. In these systems, a large perturbation can elicit a large amplitude spike or "firing," followed by a quick return to a globally attracting fixed point. The dynamical response of these systems to periodic deterministic forcing has been extensively described in both experimental and model studies. Periodic responses include n:m phase locking patterns with m firings for n forcing cycles [3]. In the space of forcing parameters, the generic arrangement of isoperiodic regions has received particular attention [2,4].

Forcing these systems with sufficiently small periodic perturbations yields trivial 1:0 steady state responses having no "spikes." This deterministically uninteresting "subthreshold" regime has received much recent attention in the context of noise-induced oscillations in neuronal networks (see, e.g., [5] and references therein) and of stochastic resonance (SR) in neurons [6]. Recent theoretical work [7–9] on SR in excitable systems has focused on the regime in which the system simply behaves as a static threshold element. For example, in "aperiodic SR" [8], signal fluctuations are slower than all system time scales; the noise intensity D optimizing the linear correlation between signal and firing rate is then independent of signal frequencies.

However, many systems are driven by higher frequency signals, and do not fully recover their resting state between firings. The effect of this recovery time scale, which by interacting with the signal time scale produces deterministic phase locking patterns, is poorly understood in the context of SR. Further, SR in its restricted sense is described as a match between signal period and an "interevent" time scale due to noise alone, and assessed by the optimization of some signal-firing correlation for some $D > 0$ [6,10]. Here we show that, for a large range of biologically relevant frequencies, the optimization of many firing statistics used in the SR context closely follows such a time-scale matching notion. Our approach focuses on the time-averaged phase locking that results from forcing with both subthreshold periodic signals and additive noise. We use the Fitzhugh-Nagumo neuron model, but our results are relevant to general noise-perturbed excitable systems [1,2], in particular to their sensitivity and tuning properties for arbitrary signals [11]. The Fitzhugh-Nagumo model with additive periodic and stochastic forcing is [8,9,12]:

$$\epsilon \frac{dv}{dt} = v(v - 0.5)(1 - v) - w + A \sin \beta t + I + \eta(t), \quad (1)$$

$$\frac{dw}{dt} = v - w - b, \quad (2)$$

$$\frac{d\eta}{dt} = -\lambda \eta + \lambda \xi(t). \quad (3)$$

The variable v is the fast voltagelike variable, w is the *slow* recovery variable, $\xi(t)$ is a zero-mean Gaussian white noise of intensity D, and η is an Ornstein-Uhlenbeck (OU) noise with variance $\sigma^2 = D\lambda$ and correlation time $t_c = \lambda^{-1}$ [13]. After a firing, recovery produces an absolute refractory time T_R during which a second firing cannot occur, followed by a longer relative refractory time during which firing requires stronger perturbations. Thus, in contrast with conventional bistable systems [6], the firing threshold or "barrier height" ΔU depends on the time since the previous firing.

Figure 1 shows the organization of steady-state periodic firing patterns in the usual forcing amplitude-period subspace. The curves depict the numerically computed boundaries between n:m locking patterns. Only three curves are shown for clarity, since the space between the 1:1 and 1:0 curves is populated by patterns with intermediate ratios [2]. The shaded region below the 1:0 curve corresponds to parameter values for which no spikes occur deterministically. The amplitude threshold for a given n:m firing is seen to depend on signal period $T = 2\pi/\beta$, and is smallest at the "best period" of the neuron $T^* \approx 1.5$. Similar resonances are found in real neurons (see, e.g., [14]); here, it arises due to the single stable "focus"-type fixed point of the two-dimensional dynamics Eqs. (1)–(3) (eigenvalues $s_\pm = -13.1 \pm i7.31$). Noise alone [15] turns the system into a stochastic oscillator

 0031-9007/98/81(18)/4012(4)$15.00

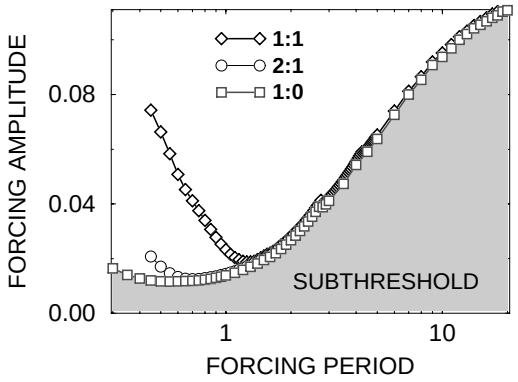

FIG. 1. Amplitude-period subspace for the periodically forced excitable system, Eqs. (1)–(3) *without noise.*

generating "spontaneous" firings. The mean interspike interval (ISI) (i.e., mean escape time to threshold) with noise only $\langle \mathrm{ISI} \rangle_{A=0}$ always decreases with increasing D, a behavior well approximated by $\langle \mathrm{ISI} \rangle \approx \exp(\Delta U/\sigma^2)$ for low D [8,16] and a power law for higher D. The "noise-induced firing" behavior is computed numerically and plotted in Fig. 2a.

With noise and a periodic signal, the response patterns depend on the interaction of two time scales: the endogenous noise-induced mean interval $\langle \mathrm{ISI} \rangle_{A=0}$ and the period of the deterministic forcing. Under these conditions, phase locking curves as in Fig. 1 need to be reinterpreted as corresponding to different time-averaged phase locking ratios, as in [17]. Thus, an n:1 pattern means an *aperiodic firing pattern* with one spike for n stimulus cycles on average. Figure 2b shows the location of the 1:1 stochastic phase locking curves (SPLC's) in the D-T subspace for three values of A. If A is subthreshold for deterministic 1:1 regardless of T ($A < 0.019$; see Fig. 1), then the D value which produces an average 1:1 decreases monotonically with increasing T. The system no longer has a best period from this point of view. Naturally, D falls to zero

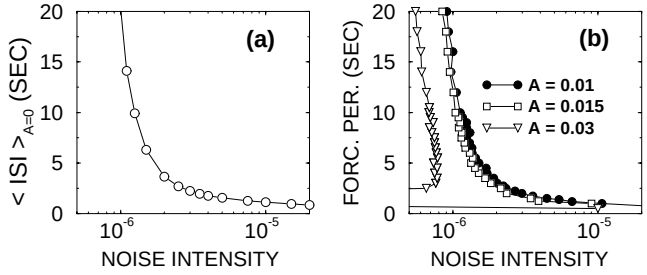

FIG. 2. (a) Mean interspike interval versus noise intensity D for Eqs. (1)–(3) *without periodic forcing*. (b) Stochastic 1:1 curves in the noise intensity-stimulus period subspace. For each sinusoidal forcing period, the noise intensity D yielding on average one firing per forcing cycle is computed. The actual values of D plotted in (b) are averages from three searches, each of which uses 100 forcing cycle realizations. Stochastic numerical integration [9] uses a time step of 0.001 sec for signal periods $T < 1.5$ sec and 0.0025 sec otherwise.

at those periods for which the signal is deterministically suprathreshold. This is seen between $T \approx 1$ and $T \approx 2.5$ for the 1:1 SPLC with $A = 0.03$, and over larger period ranges for the 2:1, 3:1 . . . SPLC's when $A = 0.015$ or 0.03 (not shown). Also, by definition, the 1:1 SPLC must converge to the curve in Fig. 2a as $A \to 0$. This is seen in Fig. 2b (see also Fig. 3a), where curves move to the right for decreasing A, implying that the average ISI with or without signal become the same.

These results set the stage for analyzing the dependence of firing statistics used in conventional SR studies on D and T and determining whether "optimal" statistics are organized according to the time-scale matching notion of SR [6,10]. The idea is to use, for each statistic studied, the same axis to plot the two time scales to be matched: the zero-signal "mean escape time" and the signal period T. Thus, the D vs $\langle \mathrm{ISI} \rangle_{A=0}$ curve in Fig. 2a is replotted (with axes interchanged) in each panel of Fig. 3, alongside optimal firing statistics curves in the presence of both signal ($A = 0.01$) and noise.

1:1 SPLC.—Figure 3a plots the noise-induced firing curve alongside the 1:1 SPLC (Fig. 2b, $A = 0.01$). This clearly shows the (trivial) matching between the spontaneous (i.e., zero signal) firing and the average 1:1 firing for small signals. We now investigate whether other statistics display similar matching.

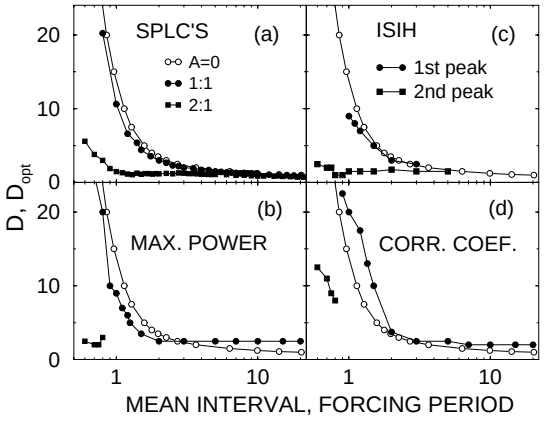

FIG. 3. Dependence on forcing period T (with $A = 0.01$) of the noise intensity D_{opt} ($\times 10^{-6}$) which optimizes firing statistics (filled symbols). The data for $\langle \mathrm{ISI} \rangle$ versus D without forcing (Fig. 2a: open circles) are plotted in each panel. (a) Stochastic phase locking curves showing, as a function of T, the value D_{opt} producing on average one firing per cycle (1:1) and per two cycles (2:1). (b) D_{opt} here yields maximal power at the forcing frequency $1/T$ in the spike train power spectrum. For $T < 0.9$, points correspond to a secondary power peak at $1/T$. (c) D_{opt} yields a maximum number of intervals of duration $\approx T$ (first peak) and $\approx 2T$ (second peak). (d) D_{opt} yields the maximum linear correlation C between the forcing and the firing probability. For $T < 0.9$, D_{opt} follows another branch. In (b)–(d), dynamical refractory effects occur for $T < 3$, and statistics with signal parallel the zero-signal mean interval. D_{opt} is independent of T in the static regime $T > 3$. Symbols are approximately two standard deviations wide.

Power spectral density.—Figure 3b compares spontaneous firing to the power spectral density at frequency $f = 1/T$ contained in the sequence of firing times. For each T, Fig. 3b plots the value $D = D_{\text{opt}}$ that maximizes this power. This curve flattens for $T > 3$ where the two curves crossover (note that the zero-signal curve always decreases). However, for $T < 3$, D_{opt} lies under, yet parallels the spontaneous firing curve. For $T < 1$, we find more than one local maximum for a given T (see also [18] in the bistable system context). In fact, due to tight phase locking, the local maxima associated with the points plotted for $T < 0.8$ have higher power than those lying on the extension of the main curve (filled circles) off scale into unrealistic noise levels. This stochastic phase locking structure will be detailed elsewhere [19].

Interspike interval histograms (ISIH's).—The equivalent to escape time distributions are the ISIH's (Figs. 4a, 4c). A local maximum around the forcing period T implies that the escape process is synchronized to this forcing. Accordingly, Fig. 3c is based on the number of intervals near integer multiples of T [12,20,21], which is also the relevant statistic to quantify *bona fide* SR in bistable systems [10]. Histogram peaks at multiples of T occur typically for Eqs. (1)–(3) if T is small, but also for any T provided D is small [9]. For each T, we estimate D_{opt} for which the number of intervals close to T is maximal. The curve D_{opt} vs T shown in Fig. 3c again closely parallels the spontaneous curve and the 1:1 SPLC over the range of forcing periods for which interval histograms indeed have a peak at T.

Intuitively, the value of D producing a maximal number of interspike intervals of duration close to T should be close to the value of D producing on average one spike per cycle. Likewise, this value of D should also be close to that which maximizes the spectral power at frequency $1/T$. For larger T the estimation of D_{opt} for the ISIH is artifactual since, before going through a maximum, the first peak is washed out by the growing exponential (Poisson) background caused by numerous firings per period (Fig. 4c). Also, for $T < 1$, no peak at T is seen since recovery prevents firings in two successive cycles. Also shown is the D_{opt} vs T for the second ISIH peak at $2T$. This curve lies below that for the first peak, as expected from SR studies in bistable [10,20] and excitable systems [12,21]. The second peak curve is similar to the 2:1 SPLC in Fig. 3a, as expected following the same intuition as above.

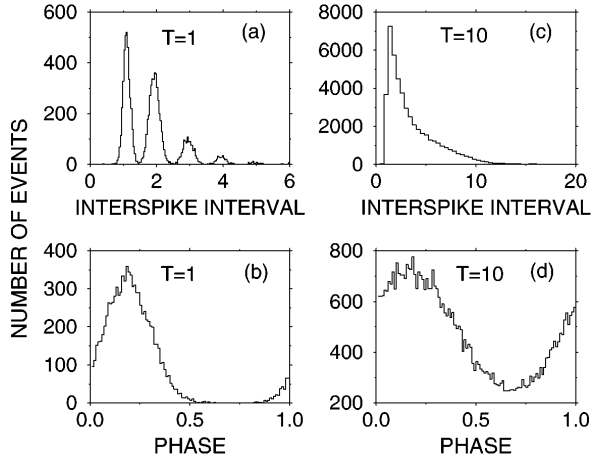

FIG. 4. Interspike interval histograms [(a),(c)] (200 bins) and cycle histograms [(b),(d)] (100 bins) for $T = 1$ sec (phase locking) and $T = 10$ sec (rate modulation). $D = 2 \times 10^{-6}$. Results were obtained from 50 realizations of 100 cycles with $A = 0.01$.

Linear correlation coefficient.—We finally consider the linear correlation coefficient C between the sine wave signal and the firing probability $P(\theta)$, where θ is a normalized signal phase [9,22]. $P(\theta)$ is estimated numerically using cycle histograms (CH's) (Figs. 4b and 4d), in which a bin corresponding to a given phase is incremented whenever a spike occurs at that phase. The value of C approaches one when the cycle histogram is well fitted by a suitably shifted sinusoid. This statistic reflects the degree to which the response of the neuron (firing rate) linearly tracks the input signal. For each T, Fig. 3d plots D_{opt} which maximizes C; this maximum is typically broad, with $C > 0.9$ for D varying over a fivefold to tenfold range, making the estimation of D_{opt} sensitive to statistical fluctuations. As in Fig. 3b, D_{opt} for larger T ($T > 3.5$) is independent of T. For $T < 3.5$, D_{opt} increases as T decreases, following the spontaneous curve from above. Note that D_{opt} here is slightly larger than those on the D vs $\langle \text{ISI} \rangle_{A=0}$ curve, due to the fact that in order to linearly track the signal there must be more that one firing per cycle. For $T < 0.9$, D_{opt} values shown are on a lower curve related to the spike train local power maxima in Fig. 3b. In fact, the latter maxima occur at D values which also maximize the first Fourier component of $P(\theta)$, which itself is the numerator of C.

It is clear that Fig. 3 highlights the parameter regions of frequency dependence for the optimal statistics, with qualitative agreement with the time scale imposed by the spontaneous firing. This is due to the interplay of time-dependent (dynamic) versus time-independent (static) properties of the firing threshold known to exist in both this model and real excitable cells. Since the firing threshold is in fact time dependent, due to the slower recovery, the extent to which the dynamic property is expressed depends on the time between a firing and the next forcing cycle. Thus for relatively long T, only static nonlinearities play a role; for shorter periods the dynamical aspect is also involved.

For small D (here, for $D < 10^{-6}$) and all T, the static nonlinearity produces "half-wave rectified" cycle histograms [9,22], i.e., $P(\theta)$ is negligible over half of the cycle. This nonlinear response, proportional to A, also produces multimodal ISIH's. Such CH's and ISIH's are similar to those shown in Figs. 4a and 4b; however, the latter were obtained for $T = 1$ and $D > 10^{-6}$, for which the dynamical nonlinearity is predominant. In the static

case, signal power increases with D because the spontaneous or "carrier" rate becomes large enough to be fully linearly modulated by the signal (Fig. 4d). Accordingly, C increases. Low noise yields the static nonlinear regime $A/\sigma^2 \gg 1$ with synchronization [20], and higher noise brings on a linear regime [18,23]. This explains why D_{opt} is independent of T in Figs. 3b, 3d for $T > 3$. This is similar to threshold dithering [9,24]: noise linearizes the transfer function relating signal to instantaneous firing rate. Signal period is longer than all system time scales in this analytically tractable regime [7–9], which in fact defines the domain of "aperiodic SR" [8].

Recovery is increasingly important for $T < 3$, promoting phase-locked firings a random number of cycles apart [9,22]. As for weak noise, this causes multimodal ISIH's (Fig. 4a) and rectified CH's (Fig. 4b). Recovery causes a strong dependence on T of the optimal statistics: a smaller T requires a larger D to overcome the "rectifications" produced by both the static and dynamic threshold properties, i.e., to bring on a linear regime. Similarly to bistable systems [10], we here find a matching [6,21] where D_{opt} follows signal frequency, paralleling the behavior of the spontaneous firing with D. Subharmonic resonances also appear (at lower D in Fig. 3), although, in contrast to bistable systems, T_R imposes a sharp boundary beyond which 1:1 firing is not possible.

The full excitable dynamics introduces noise-induced phenomena not found in simpler static threshold models of such systems. Dynamical and static threshold properties, and time scales due to noise and signal, determine which phenomenon is expressed by the noise.

Supported by NSERC (Canada) and NIMH (USA) (Grant No. MH50064). Early contributions by J. Müller-Gerking are appreciated as well as useful discussions with A. Bulsara, L. Gammaitoni, J. Levin, and P. Jung.

[1] See, e.g., Focus issue: From Oscillations to Excitability—A Case Study in Spatially Extended Systems, edited by S. C. Müller, P. Coullet, and D. Walgraef [Chaos **4** (1994)].

[2] L. Glass and M. C. Mackey, *From Clocks to Chaos: The Rhythms of Life* (Princeton University Press, Princeton, NJ, 1988).

[3] J. Nagumo and S. Sato, Kybernetik **10**, 155 (1972); S. Rajaseker and M. Lakshmanan, Physica (Amsterdam) **32D**, 146 (1988).

[4] D. R. Chialvo and J. Jalife, Nature (London) **330**, 749 (1988); M. Feingold *et al.*, Phys. Rev. A **37**, 4060 (1988); J. C. Alexander *et al.*, SIAM J. Appl. Math **50**, 1373 (1990).

[5] C. Kurrer and K. Schulten, Phys. Rev. E **51**, 6213 (1995).

[6] K. Wiesenfeld and F. Moss, Nature (London) **373**, 33 (1995); A. Bulsara and L. Gammaitoni, Phys. Today **49**, 39 (1996).

[7] K. Wiesenfeld *et al.*, Phys. Rev. Lett. **72**, 2125 (1994); P. Jung, Phys. Rev. E **50**, 2513 (1994).

[8] J. J. Collins *et al.*, Phys. Rev. E **52**, R3321 (1995).

[9] D. R. Chialvo *et al.*, Phys. Rev. E **55**, 1798 (1997).

[10] L. Gammaitoni *et al.*, Phys. Rev. Lett. **74**, 1052 (1995).

[11] Collins *et al.*, Nature (London) **376**, 236 (1995); J. E. Levin and J. P. Miller, Nature (London) **380**, 165 (1996); C. Ivey, V. Apkarian, and D. R. Chialvo, J. Neurophysiol. **79**, 1879 (1998).

[12] A. Longtin, J. Stat. Phys. **70**, 309 (1993).

[13] For all figures, parameters are $I = 0.04$, $b = 0.15$, $\epsilon = 0.005$, $t_c = 10^{-3}$, the threshold is 0.5, and a firing is counted only if separated from a previous one by at least $T_R = 0.4$ sec (equivalent to $\approx$1 msec in real time).

[14] R. Guttman *et al.*, Biophys. J. **14**, 941 (1974).

[15] Noise is assumed to be due to ionic conductance fluctuations or synaptic activity that depend weakly on the signal.

[16] A. S. Pikovsky and J. Kurths, Phys. Rev. Lett. **78**, 775 (1997).

[17] L. Glass *et al.*, J. Theor. Biol. **86**, 455 (1980). For near and above threshold signals, we have found Devil's staircases in mean frequency vs D plots, as in B. Shulgin *et al.*, Phys. Rev. Lett. **75**, 4157 (1995) for a bistable system in one dimension.

[18] P. Jung and P. Hänggi, Phys. Rev. A **44**, 8032 (1991).

[19] The signal-to-noise ratio (peak height divided by noise floor under the peak) is maximized by $D_{\text{opt}} \approx 2 \times 10^{-6}$ for $T > 1.1$; $D_{\text{opt}} < 10^{-6}$ until $T < 0.5$. Noise floor variations with D are complicated by T_R and noise-induced limit cycles [12,16].

[20] L. Gammaitoni *et al.*, Phys. Rev. Lett. **62**, 349 (1989); T. Zhou *et al.*, Phys. Rev. A **42**, 3161 (1990).

[21] D. R. Chialvo and V. Apkarian, J. Stat. Phys. **70**, 309 (1993); A. R. Bulsara *et al.*, Phys. Rev. E **53**, 3958 (1996).

[22] A. S. French *et al.*, Kybernetik **11**, 15 (1972).

[23] M. I. Dykman *et al.*, Phys. Lett. A **193**, 61 (1994).

[24] H. Spekreijse and H. Oosting, Kybernetik **7**, 22 (1970); L. Gammaitoni, Phys. Rev. E **52**, 4691 (1995).